Electronic Supplementary Information

Flexible humidity sensors composed of graphite-like carbon micro-pinecone arrays

Tomohiko Nakajima,* Takako Nakamura and Tetsuo Tsuchiya

Advanced Coating Technology Research Center, National Institute of Advanced Industrial Science and Technology, Tsukuba Central 5, 1-1-1 Higashi, Tsukuba, Ibaraki 305-8565, Japan.

Temperature variations during laser irradiation can be described by the heat diffusion equation simplified to describe one-dimensional heat flow:[1]

$$\rho C \frac{\partial T}{\partial t} = \kappa \frac{\partial^2 T}{\partial z^2} + \alpha I(z,t)$$

where T is the temperature function at time t and depth z, ρ is the mass density, C is the specific heat capacity, α is the optical absorption coefficient, κ is the thermal conductivity, and $I(z,t)$ is the laser power density. The laser power $I(z,t)$ is given by:

$$I(z,t) = I_0(t) \cdot (1-r) \cdot \exp(-\alpha z)$$

where r is the reflectance. The contribution from the incremental absorbance of the films caused by reflectance at the substrate surface was also included in the laser power distribution. $I_0(t)$ is described as a smooth pulse approximated by:

$$I_0(t) = I_0 \cdot \left(\frac{t}{\tau}\right)^{\beta} \cdot \exp\left(\beta\left(1 - \frac{t}{\tau}\right)\right)$$

where I_0 is the incident pulse power density, τ is the pulse duration (KrF: 26 ns), and β determines the temporal pulse shape (KrF: 6.0). We carried out numerical simulations for the temperature variation for the excimer laser irradiation process using a difference approximation based on the above equations. The initial conditions were $T = 25$ °C at $t = 0$ s and $T = 25$ °C at the bottom of the substrate. The boundary condition was $\kappa \frac{\partial T}{\partial z} = 0$ at the interfaces. The physical constants used in the calculations are listed in Table S1.

Table S1 Physical properties used in numerical simulations.[2–4]

Material	α / cm^{-1}	r	κ / Wcm^{-1}K^{-1}	ρ / g cm^{-3}	C / Jg^{-1}K^{-1}
Polyimide	2.6×10^5	0.09	1.2×10^{-3}	1.42	1.09
Graphite	1.776×10^4	0.0377	1.124	2.26	0.72
SiO_2	0.83	0.08	0.015	2.20	0.67

Figure S2 shows the monitoring setup for the humidity sensing property under various gas flow: humidified/dried N_2, O_2 and H_2/Ar. The humidity source was made from water bubbling.

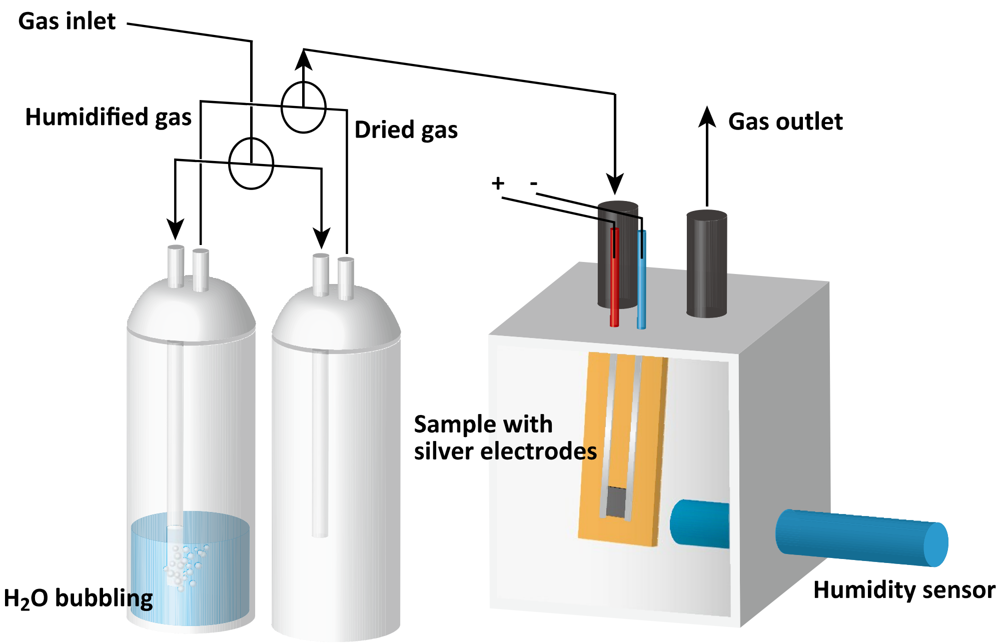

Fig. S1: The monitoring setup for the humidity sensing property.

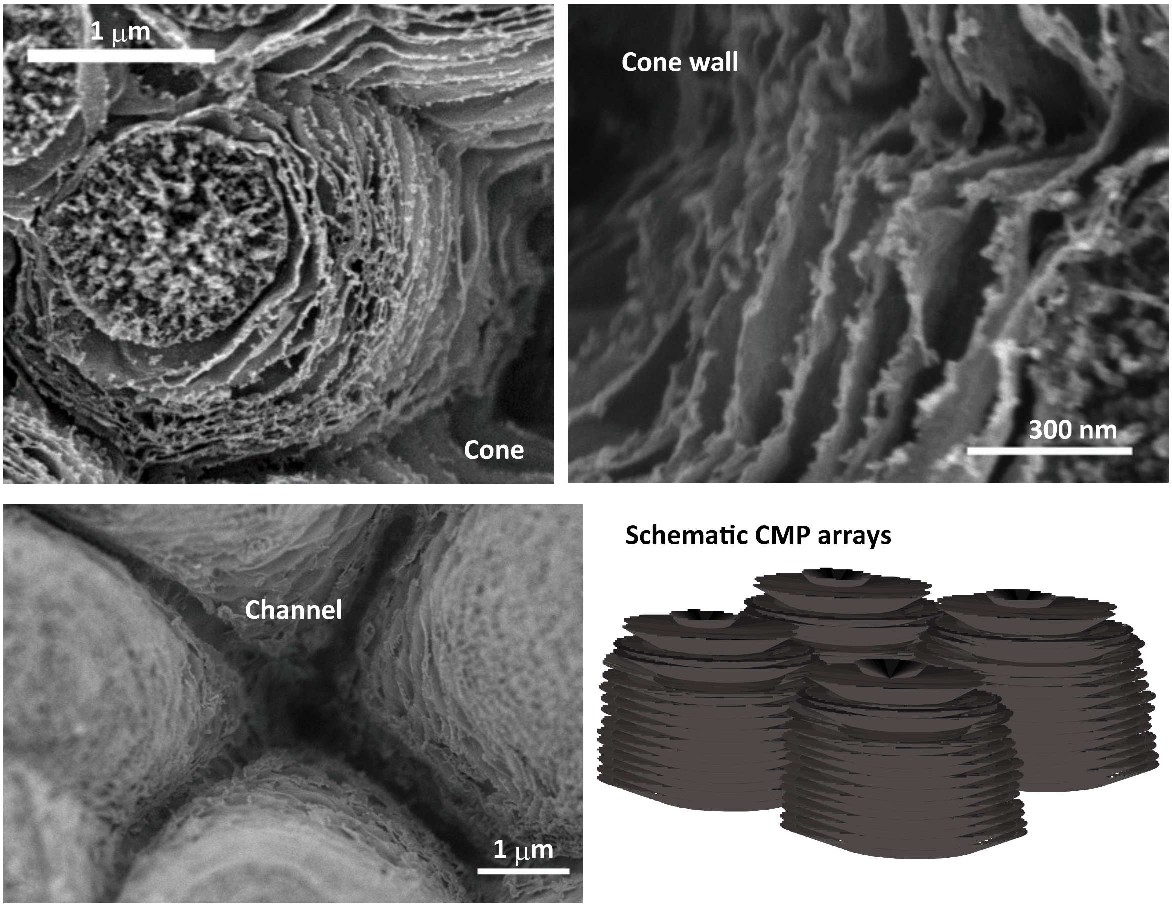

Fig. S2: The FESEM images for the CMP arrays prepared at 200 mJ·cm^{-2} and schematic illustration of CMP arrays.

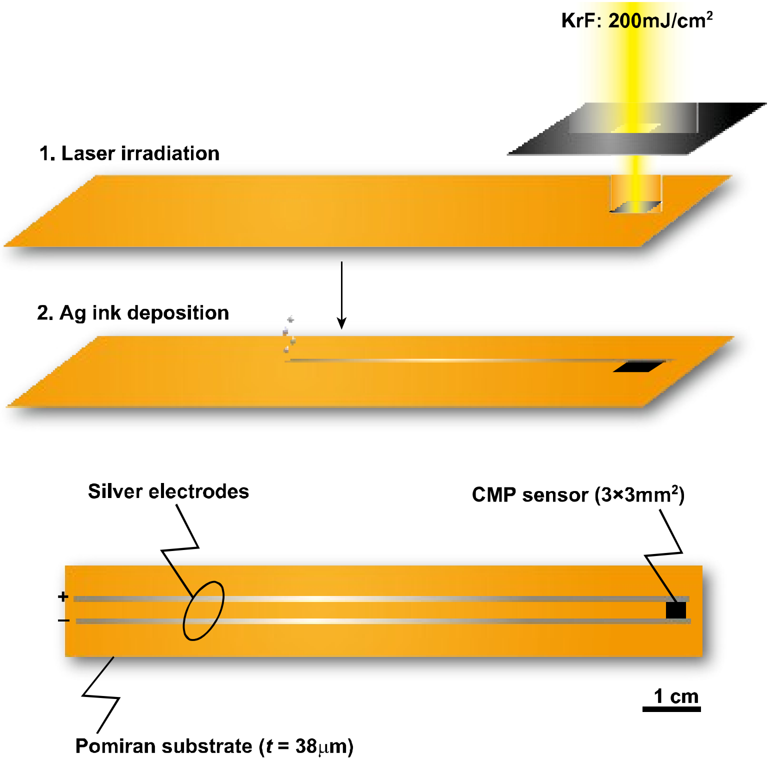

Fig. S3: Schematic illustrations for the preparation procedure and size of the CMP array humidity sensor.

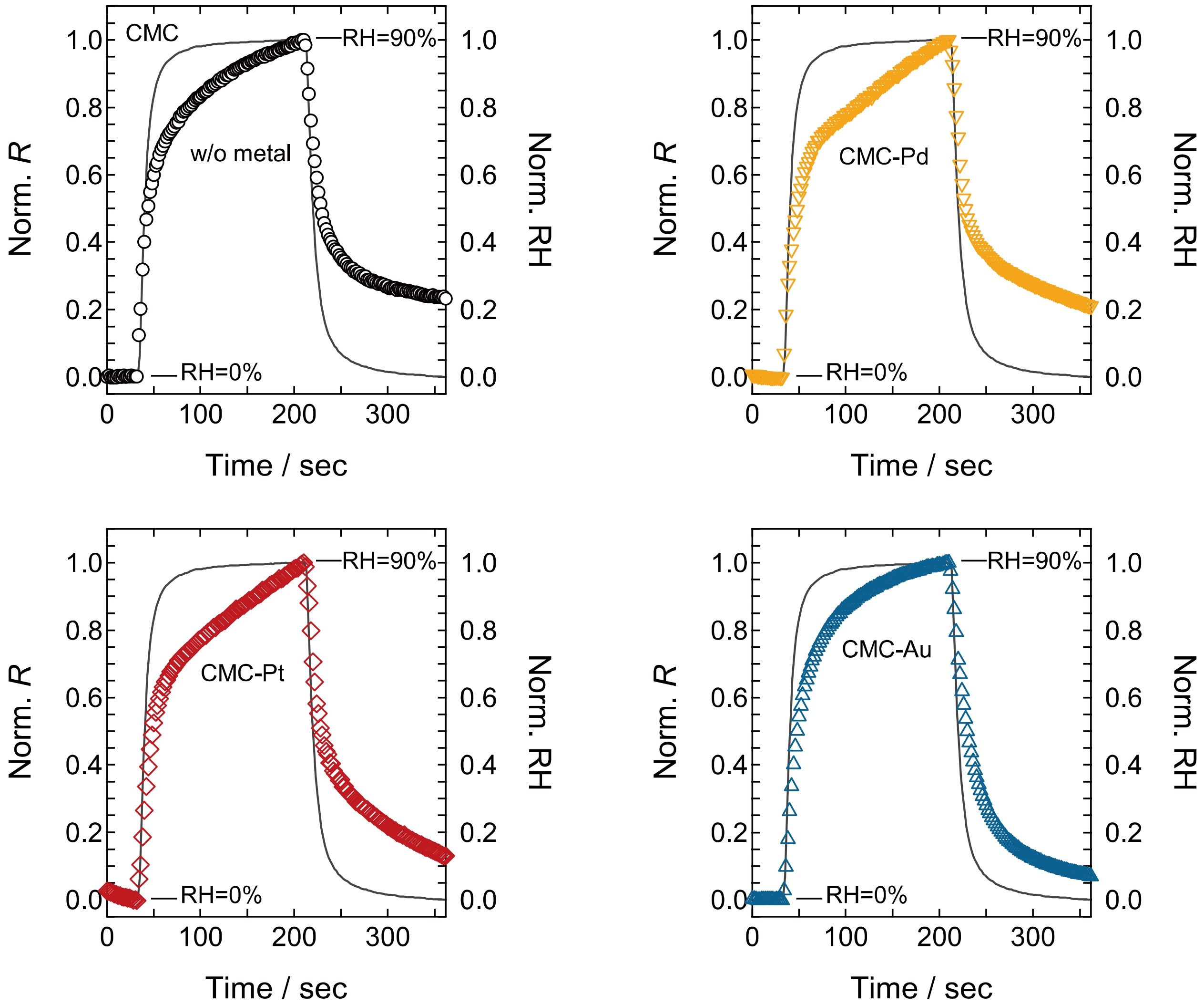

Fig. S4: The time course of normalized *R* for CMC and CMC-M (M: Pd, Pt and Au). The dotted line represents normalized RH curve monitored by commercial humidity sensor. In the time course measurements, the gas flow was changed as follows: dried N_2 (0–30 s) – humidified N_2 (30–210 s) – dried N_2 (210–360 s).

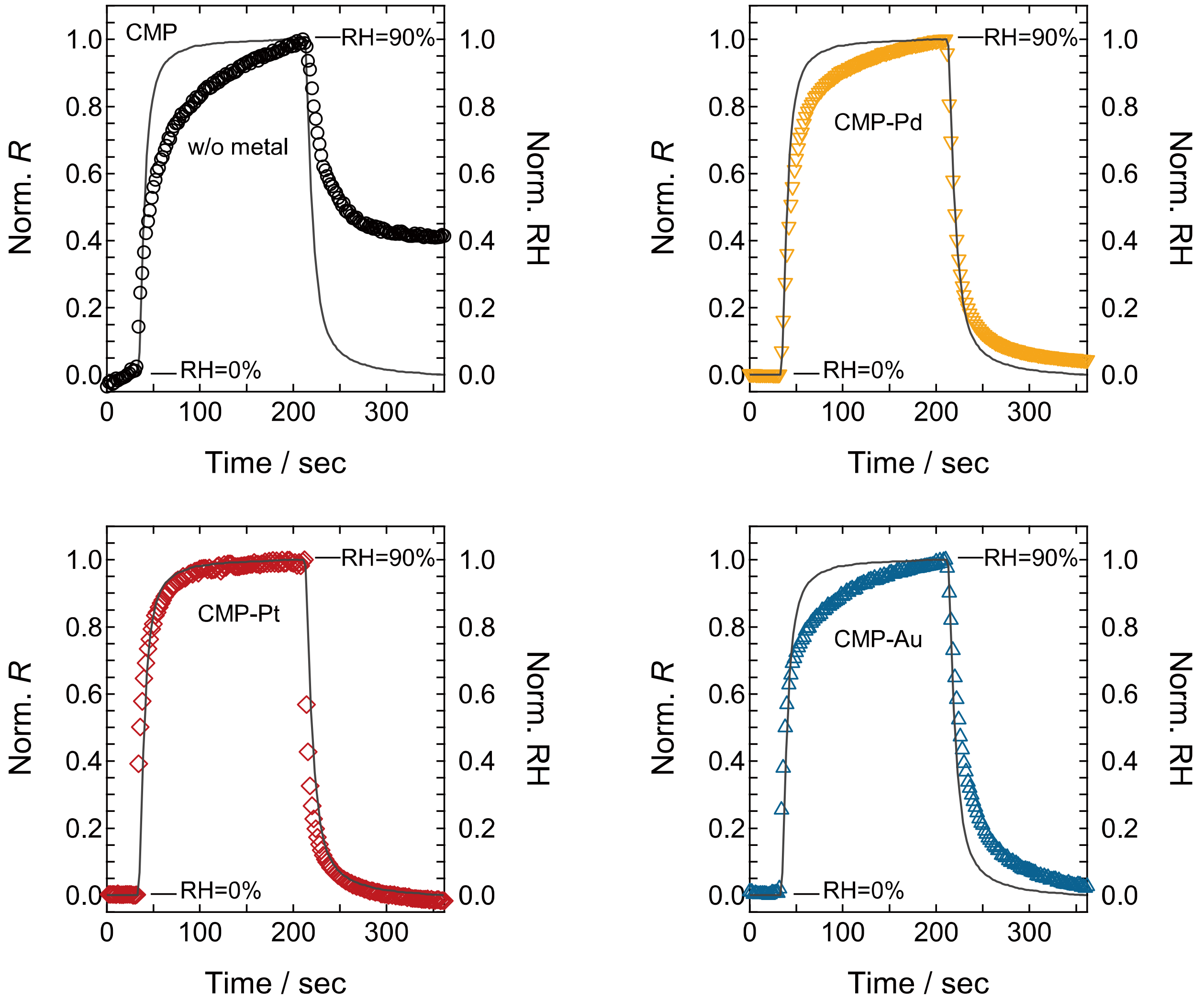

Fig. S5: The time course of normalized *R* for CMP and CMP-M (M: Pd, Pt and Au). The dotted line represents normalized RH curve monitored by commercial humidity sensor. In the time course measurements, the gas flow was changed as follows: dried N_2 (0–30 s) – humidified N_2 (30–210 s) – dried N_2 (210–360 s).

References

1 D. Bäuerle,: *Laser Processing and Chemistry* (Springer-Verlag Berlin Heidelberg New York 2000)
2 http://www.dupont.com/content/dam/dupont/products-and-services/membranes-and-films/polyimde-films/documents/DEC-Kapton-summary-of-properties.pdf
3 https://www.entegris.com/resources/assets/6205-7329-0513.pdf.
4 T. Nakajima, T. Tsuchiya and T. Kumagai, *Cryst. Growth Des.*, 2010, **10**, 4861.
5 *Materials Safety Data Sheet Solution Center:* http://www.msds.com/.